Surface Science 177 (1986) 191–206
North-Holland, Amsterdam

ADSORPTION OF H_2O ON CLEAN AND ON BORON-CONTAMINATED Rh SURFACES

János KISS and Frigyes SOLYMOSI

Reaction Kinetic Research Group of the Hungarian Academy of Sciences
and Institute of Solid State and Radiochemistry,
University of Szeged, P.O. Box 105, H-6701 Szeged, Hungary

Received 7 January 1986, accepted for publication 9 July 1986

The adsorption and dissociation of H_2O on Rh(111) and Rh foil surfaces have been studied in UHV using Auger electron, electron energy loss (in the electronic range) and thermal desorption spectroscopy. H_2O adsorbs weakly on clean Rh samples at 110 K. The adsorption is accompanied by the appearance of a broad loss feature at 14–14.5 eV. At higher exposures new losses appeared at 8.6 and 10.5 eV. The desorption of H_2O took place in two stages, with $T_p = 183$ K (β, chemisorption) and 158 K (α, multilayer formation). There was no indication of dissociation of H_2O on a clean Rh(111) surface. Similar results were obtained for a clean Rh foil. However, when small amounts of boron segregated on the surface of Rh, they exerted a dramatic influence on the adsorptive properties of this surface and caused the dissociation of H_2O. This was exhibited by the formation of H_2, by the buildup of surface oxygen, by the appearance of an intense new loss at 9.4 eV, identified as B–O surface species, and by the development of "boron-oxide"-like Auger fine structure.

1. Introduction

We recently found that Rh supported on TiO_2 effectively catalyses the $H_2O + CO$ reaction to produce hydrocarbons and oxygenated compounds [1]. In addition, Rh/TiO_2 proved to be active in photocatalytic water splitting [2,3] and in the photocatalytic $H_2O + CO_2$ reaction [4,5]. In order to understand the role of Rh in the activation of the water molecule, and to evaluate the effect of the TiO_2 support, it appeared inevitable to learn more about the interaction of H_2O with Rh surfaces. Apart from a short conference abstract [6], no literature data are to be found on adsorption of H_2O on Rh surfaces under UHV conditions.

The interaction of H_2O with clean metal surfaces has been the subject of a number of detailed studies. Water vapour undergoes reversible molecular adsorption and desorption on Pt(111) and (100) [7–14], Pd(100) [15] and Ru(001) surfaces [16–19]. Dissociation occurs to a small extent (less than 6%) on Ir(110) [20]. A more significant dissociation, with the formation of hydro-

0039-6028/86/$03.50
(North-Holland Physics Publishing Division)

gen, has been observed on stepped Re and Re(0001) [21], Al(111) and (100) [22], Ti(001) and Fe(110) [24] surfaces. The dissociation of H_2O exhibits a face specificity on Ni [25–28], Re [21] and Co [29] surfaces. On Ag(110) [30] and Cu(110) [31–33], H_2O adsorption is molecular.

In the present study the adsorption of H_2O is investigated on two Rh samples, Rh(111) and a polycrystalline Rh foil, by means of AES, EELS (in the electronic range) and TDS methods. Special emphasis is paid on the effects of boron impurity.

We recently observed that boron impurity segregating to a Rh surface can greatly alter its reactivity towards N-containing moieties such as N, CN and NCO [34–36]. A possible reason for this phenomenon is that boron forms a very strong bond with N, which can promote rupture of the C–N bound at high temperature and can prevent the associative desorption of N below 1100 K. We have also presented strong evidence that boron impurity on Rh surfaces (Rh(111) and Rh foil) can cause the dissociative adsorption of CO_2 at 300 K, which does not occur to a detectable extent on clean Rh surfaces [37, 38]. We expected a similar influence of boron in the case of H_2O adsorption on Rh, too.

2. Experimental

The experiments were performed in a stainless steel UHV chamber equipped with several gas inlets, a single pass CMA (PHI) for AES, a 3-grid retarding field analyzer (VG) for LEED and a quadrupole mass analyzer (VG) to monitor the gas-phase composition. The vacuum system was evacuated with ion pumps and a titanium getter. The sample mounted on a manipulator can be cooled to 100–110 K and heated up to 1300 K.

For electron energy loss spectra the gun of CMA was used as a primary electron source with an energy of 70 eV and a beam current of 0.1–1.0 μA. The backscattered electrons were analyzed with CMA. A modulation voltage of 0.1 eV was found to be the optimum for the used system. The velocity of taking a spectrum was varied between 0.4 and 4 eV/s. The exact positions of the peak maxima of energy losses were determined by a Keithley electrometer. Electron energy loss spectra were taken in $\mathrm{d}N(E)/\mathrm{d}E$ form.

Two different Rh samples were used, a Rh(111) disk shape crystal (6×1 mm, Material Research Co., 99.99% purity) and a polycrystalline Rh foil (10×10 mm and 0.127 mm thick, Hicol Co., 99.9% purity). The initial cleaning procedure has been described previously [34–38]. It consisted of ion bombardment and annealing at 1270 K. As this Rh(111) sample has been used in a number of previous studies, its cleaning required no oxygen treatment. The major contaminants of Rh foil were B, P, S and C. The P, C and S were easily removed, but no complete elimination of boron was achieved even after several cleaning cycles. The final thermal treatment in this case was performed at 700 K.

H_2O was distilled three times before use; it was further purified by several cycles of freezing and pumping until the mass spectrometer displayed only water peaks. To avoid contamination from the walls of the UHV chamber, H_2O was introduced into the chamber through a stainless steel capillary with a diameter of 0.8 mm.

Segregation of boron was achieved by annealing the Rh foil at 750–1200 K. The level of surface boron is characterized by the relative intensity of the boron Auger signal, $R_B = B_{178}/Rh_{302}$. A crude calculation based on relative intensities of Auger signals (Handbook of Auger electron Spectroscopy) resulted in a value of 3×10^{14} borons/cm^2 at $R_b \approx 0.09$.

3. Results

3.1. Rh(111) surface

3.1.1. AES and TDS measurements

Fig. 1 illustrates the Auger electron spectrum of a cleaned Rh(111) surface. It exhibits only signals due to Rh. By careful examination of the energy region of boron at 170–180 K, we could detect only a break or a slight shoulder at 178 eV. This shoulder is practically always present on the AES of clean Rh samples. Exposure of this surface to 100 L H_2O at 300 K produced no change

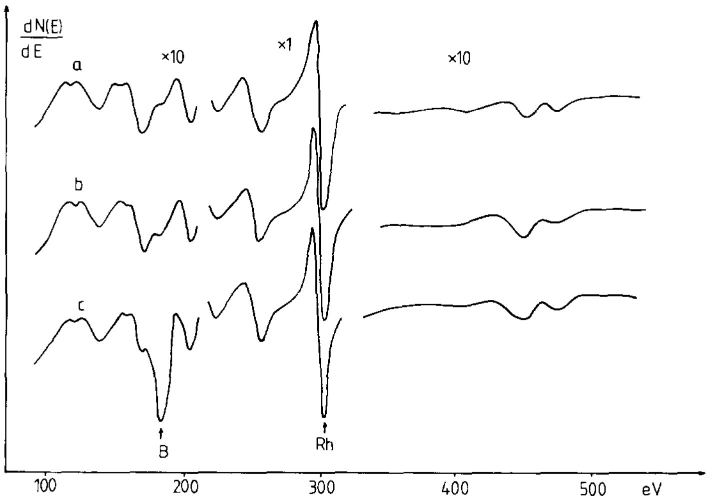

Fig. 1. Auger spectra of Rh samples: (a) clean Rh(111) ($R_B < 0.003$); (b) clean Rh foil ($R_B \sim 0.003$); (c) Rh foil contaminated with boron ($R_B \sim 0.04$).

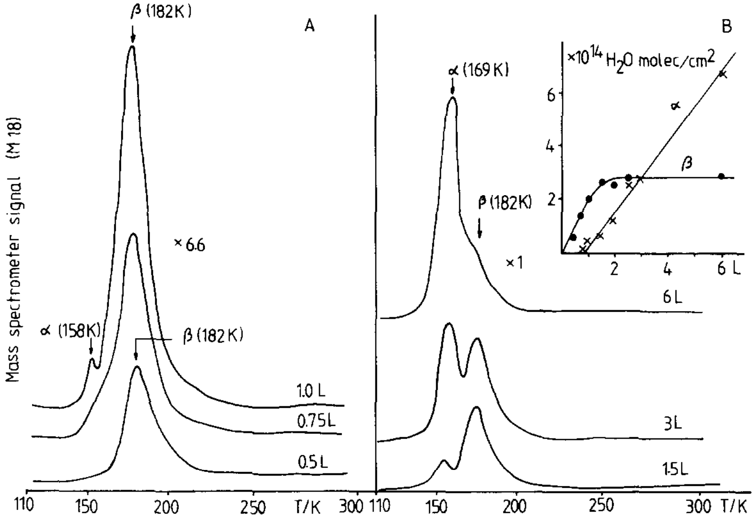

Fig. 2. (A) Thermal desorption spectra following H_2O adsorption on Rh(111) at 110 K. (B) Surface concentration of H_2O adsorbed in α and β states as a function of H_2O exposure on a clean Rh(111) surface. Heating rate was 10 K s^{-1}.

in the Auger spectrum. In harmony with this, we could not detect any desorption products after exposure.

However, when H_2O was adsorbed at 110 K, two adsorption states of H_2O were detected. Fig. 2 shows a series of TD spectra in the low- and high-exposure regions. Lower exposures produced a single peak at 182–185 K, denoted by β. From 1 L, a new peak, denoted by α, developed at 158 K.

The amount of H_2O desorbed in the β state increased linearly with the exposure up to 1.5 L, suggesting a mobile precursor model of adsorption (fig. 2). This state became saturated at about 2.5–3 L. Quantitative analysis of the peak areas, taking into account the pumping rate and the mass spectrometer and ion gauge sensitivity for H_2O, demonstrated that in this state the amount of adsorbed H_2O was approximately 3×10^{14} H_2O molecules/cm^2, which corresponds to 0.19 ML surface concentration (1 ML = 1 monolayer = 1.59×10^{15} molecules/cm^2 = the density of surface atoms on Rh(111)).

The lower-temperature α peak at 158 K appeared at 65% saturation of the first layer (0.15 ML). The peak maximum shifts to higher temperature with increasing coverage. This indicates a zero-order process, which is in harmony with the sharp drop of the high-temperature edge of this peak (fig. 2). As saturation of this state is not attained, even at 10 L H_2O exposure, we identify this state with multilayer H_2O.

For a calculation of the activation energy for desorption in the α state, the logarithm of the desorption rate at the leading edge was plotted against $1/T$: we obtained 43 kJ/mol.

The activation energy for desorption in the β stage was calculated by various methods. If it was estimated on the basis of simple first-order kinetics, assuming a pre-exponential factor of 10^{13} s^{-1}, we obtained a low value of 45 kJ/mol. Analysis of the data with the method of Chan et al. [39] or by the half order kinetics resulted in lower values.

It is important to point out that no H_2 desorption was observed from a clean Rh(111) surface after H_2O adsorption.

3.1.2. EELS studies

The adsorption of H_2O was also followed by EELS measurements. The EEL spectrum of a clean Rh(111) surface showed the same losses, at 2.6, 5.2–6.6, 17.8–18.6 and 24.5 eV (fig. 3a), as observed in our previous works [36,40,41]. On exposure of this surface to H_2O at 110 K, a broad loss feature developed at 14–14.5 eV. No other loss was observed below 1.5 L H_2O exposure. Above this value, i.e. when the multilayer developed, new losses appeared at 8.4 eV and at 10.5 eV. Their intensities increased with the rise of H_2O exposure. At the same time, the intensity of the intrinsic loss of Rh at 5.2–6.6 eV clearly attenuated (fig. 3a).

In the subsequent measurements, a Rh(111) sample saturated with H_2O at 110 K was heated to the designated temperature at a rate of 10 K/s, kept there for 1–2 s, and then allowed to recool to 110 K before its spectrum was recorded. Fig. 3b compares some spectra obtained in this way. The 8.4 and 10.5 eV losses started to attenuate at the beginning of heating, and disap-

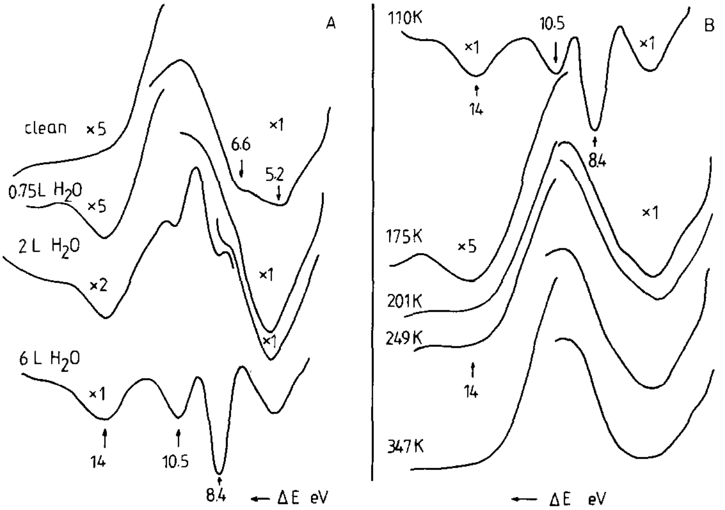

Fig. 3. EEL spectra of Rh(111) at different H_2O exposures at 110 K (A) and after heating the sample exposed to 6 L H_2O to different temperatures (B). $E_p = 70$ eV, $I_b = 0.2$–0.5 μA.

peared at 175 K. The 14–14.5 eV loss was more stable; it was eliminated at about 200 K.

3.2. Rh foil containing boron impurity

3.2.1. Adsorption at 100 K

The experiments were repeated with Rh foil. The purity of this sample is lower than that of Rh(111) and it required an extensive cleaning procedure to reduce the boron level to a minimal value. The lowest value we could attain for the Auger intensity ratio $R_B = B_{178}/Rh_{302}$, was ~ 0.003 (fig. 1). The main characteristic features of the interaction of H_2O with this surface agreed quite well with those registered for a clean Rh(111) surface. The peak temperatures for the α and β states remained practically unaltered on the boron-containing Rh surfaces, too. The amount of H_2O desorbed in the β state, however, decreased with the increase of R_B (fig. 4); for $R_B = 0.08$ it was 1.5 times less than that from the clean Rh foil. A basically new feature was the formation of two high temperature states with $T_p = 320$ and 370 K (fig. 4c). The amount of H_2O desorbed in these states was only a fraction of the β state (about 3%) and can be only detected by highly sensitive TDS measurements.

Another new feature was the evolution of H_2 ($T_p \sim 367$ K), which was never observed in the case of clean Rh(111) or Rh foil surfaces (fig. 5). The peak temperature of H_2 desorption closely approached the highest values

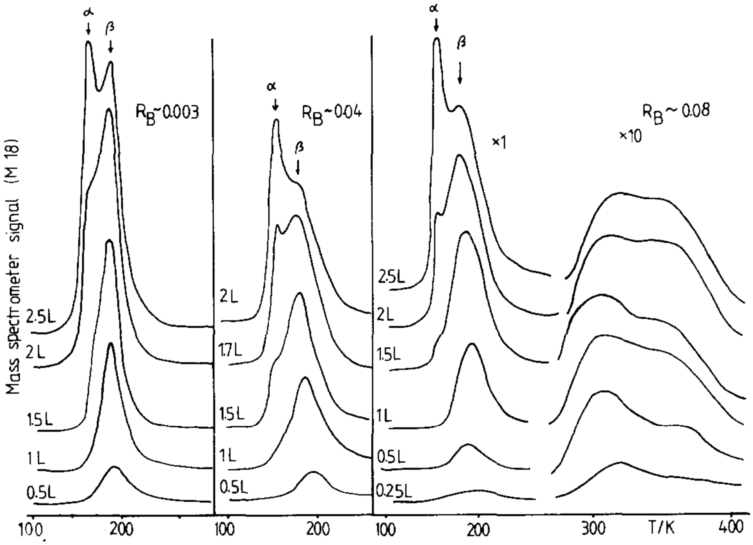

Fig. 4. Thermal desorption spectra following H_2O adsorption on the Rh foil of different boron impurity levels at 110 K.

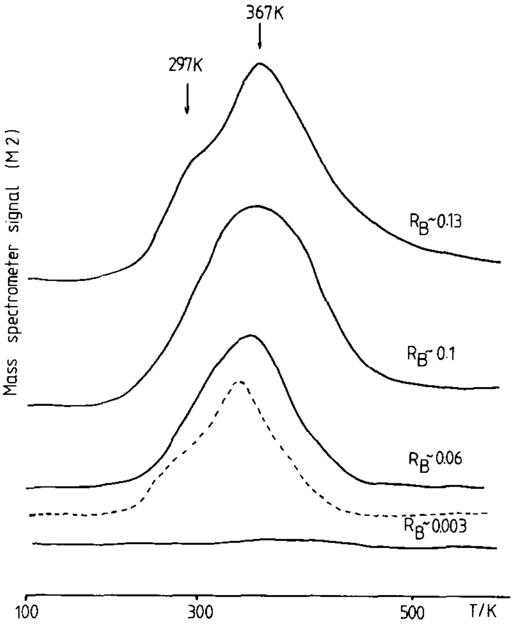

Fig. 5. Formation of H_2 following 10 L of H_2O exposure at 110 K on Rh foil of different boron impurity levels. The dashed line represents the desorption of H_2 following H_2 adsorption on a clean Rh foil ($R_B \sim 0.003$).

obtained after H_2 adsorption on Rh(111) and Rh foil surfaces at low coverages ($T_p \sim 360$–400 K) [42–45]. This result suggests that a portion of the adsorbed H_2O dissociates during the adsorption or in the course of the heating of the adsorbed layer, very probably due to the effect of boron impurity on the surface. As the data in fig. 5 show, an increase in the R_B values, through annealing of the Rh foil at 850–1200 K, enhanced the amount of H_2 evolved. At the highest boron impurity level, a second H_2 desorption peak developed at 295 K. The amount of H_2 evolved was calculated to be $\sim 1 \times 10^{14}$ molecules/cm^2, which means that at most $\sim 25\%$ of chemisorbed H_2O decomposed on the surface.

The EEL spectra of a clean, and of a boron-contaminated Rh foil showed the same losses as were observed for clean Rh(111). There was no additional losses due to the presence of boron on the surface. Exposure of these surfaces to H_2O at 110 K produced losses similar to those in the case of Rh(111) (fig. 6). The intensity of the 14 eV loss was somewhat higher at saturation of the β state (2.5–3 L) in the presence of boron impurity ($R_B \sim 0.08$) than for the clean Rh foil.

However, a significant difference was found when the EEL spectra were

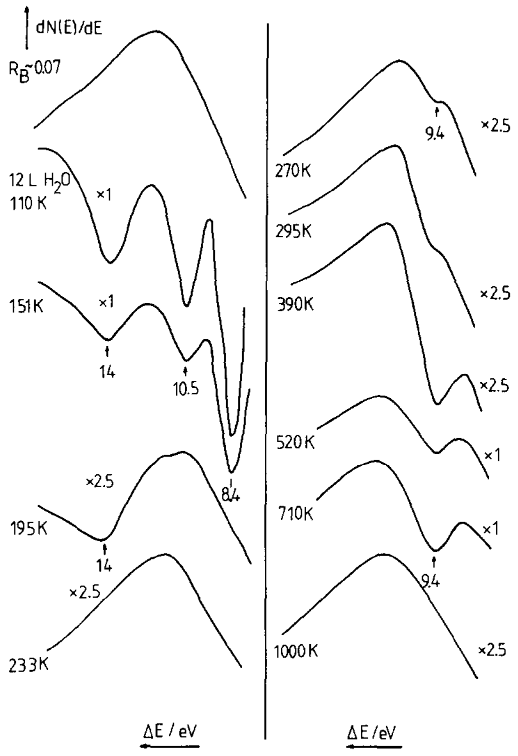

Fig. 6. EEL spectra of Rh foil (R_B ~ 0.08) taken after heating the sample exposed to 12 L H_2O at 110 K to different temperatures.

registered after stepwise heating (at 10 K/s) of the adsorbed layer to higher temperatures (fig. 6). The development of a new loss at 9.4 eV in the EEL spectrum of boron-contaminated Rh surfaces can be clearly established at 270 K. The intensity of this loss attained a maximum at 640–700 K and decreased to an undetectable level above 950 K. In this case, the sample was kept at the designated temperature for 1–2 s. However, a significant increase in the intensity of the 9.4 eV loss can be obtained at lower temperature if the sample is kept there for sufficient time (see next section). Similarly to the clean surface the 10.5 and 8.4 eV losses were detectable up to 175 K. The loss at 14.0–14.5 eV was present up to 210 K.

3.2.2. Adsorption at 300–420 K

In this case we examined the interaction of H_2O with a boron-containing Rh surface by high-resolution Auger spectroscopy in the boron signal range 140–200 eV. The elemental boron KLL spectrum (fig. 7) shows an asymmetric feature in the $dN(E/)/dE$ mode; the positive and negative wings have very

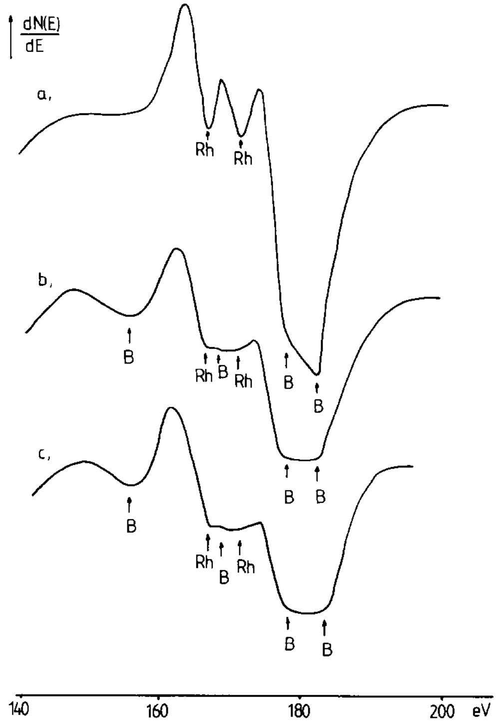

Fig. 7. High-resolution Auger spectra of boron-contaminated Rh foil ($R_B \sim 0.07$) in the boron Auger signal range: (a) before H_2O adsorption, (b) after 50 L of H_2O exposure at 300 K, (c) sample (b) heated to 660 K ($E_p = 2.5$ keV, $I_b = 0.5$ μA, $V_{mod} = 1$ V).

different intensities. The peak displays two minima, at 179 and 182 eV. After the adsorption of 50 L of H_2O at 300 K, the intensities of the boron signals at 179 and 182 eV markedly decreased and two additional peaks developed, at 157 and 168–172 eV. The latter peak was superimposed on the Rh Auger structure present at 166 and 171 eV. When the H_2O-exposed sample was heated, no changes occurred in the structure or in the intensities of the Auger signals up to 660 K. The original shape of the elemental boron feature was regained after heating to about 1000 K.

Following the adsorption of H_2O on boron-containing Rh at 300 K, we also observed the high-temperature adsorption states of H_2O at 360 and 460 K. It can be seen from fig. 8a that the development of these states is strongly dependent on the surface concentration of boron. The amount of H_2O desorbed from a saturated layer at $R_B = 0.07$ corresponds to about 1.0×10^{13} molecules/cm^2. The formation of H_2 also occurred in this case with $T_p = 392$ K (fig. 8c). On interruption of the heating after desorption of H_2 at 640 K, the

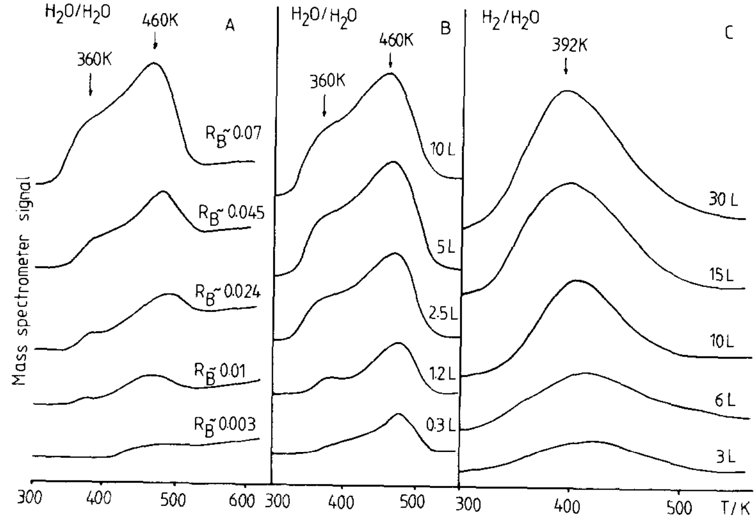

Fig. 8. (A) Thermal desorption spectra following 10 L H_2O adsorption on Rh foil of different boron impurity levels at 300 K. (B) Effect of H_2O exposures at 300 K on the desorption of H_2O from Rh foil ($R_b \sim 0.07$). (C) Formation of H_2 following 10 L of H_2O exposure at 300 K ($R_B \sim 0.07$).

oxygen Auger signal was detected at 513.7 eV. On exposure of this surface to H_2O, less H_2 was formed during the thermal desorption. After the third H_2O exposure, the H_2 produced was only just detectable.

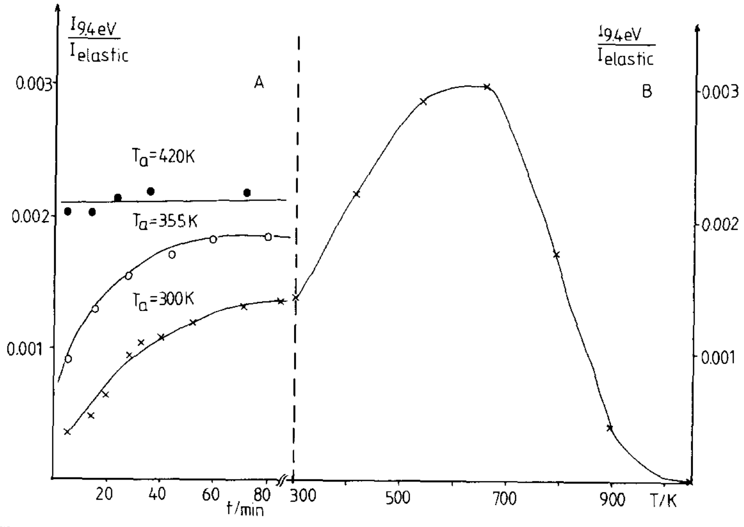

Fig. 9. Changes in the intensity of the 9.4 eV loss at different temperatures (A) and after heating the sample exposed to H_2O at 300 K to higher temperatures (B). Heating rate was ~ 10 K/s and the sample was kept at the designated temperature for ~ 2 s.

H_2O adsorption at 300 K produced a perceptible loss feature at 9.4 eV in the EEL spectrum only at higher H_2O exposure (< 10 L). Intensification of this loss was achieved when the sample was kept at 300 K for a longer period, or was heated to higher temperature, or a higher adsorption temperature was applied (fig. 9).

4. Discussion

4.1. H_2O adsorption and desorption on a clean Rh(111) surface

H_2O adsorbes readily on the Rh(111) surface at 110 K. By means of thermal desorption measurements we distinguished two adsorption states. The more strongly bonded one (T_p = 182–185 K) can be attributed to the weakly chemisorbed first monolayer (β state). From the relationship between surface coverage (β) and exposure, it appears that the sticking coefficient is constant for submonolayer coverages (fig. 2). From this correlation the sticking probability is estimated to be near unity (0.78). Similar values were obtained in the case of Pt(100) [11], Ir(110) [20] and Cu(110) surfaces [33]. The amount of H_2O desorbed in this state increased linearly with exposure up to 1.5 L, suggesting a mobile precursor model of adsorption. From the shape of the desorption peak (β), we may assume an attractive interaction between adsorbed molecules: the full width of the desorption peak at half maximum is only 15–22 K (fig. 2). Calculation of the activation energy for desorption of the β state on the basis of first-order kinetics gives a low value, 45 kJ/mol. Similar values (42–51 kJ/mol) were obtained in other cases [8,15,19,25] when a first-order desorption process was assumed. We note that in the majority of cases, the peak relating to desorption of the first layer is shifted to higher temperatures as the coverage increases. The fact that no shift was observed for the β state in the present case may be due to the relatively low coverage (saturation of this state is attained already at 0.2 ML), which prevented the recording of a sufficient number of desorption curves. The same situation existed for the Pd(100)–H_2O [15] system, where saturation of the first layer occurred at 0.25 ML. Similar behaviour was exhibited by Re(0001) [21], on which no shift of the β state was observed within the experimental accuracy. Reconstruction of the adsorbed layer, changes at the adsorption sites, or the beginning of dissociation of water during the desorption were proposed as possible reasons. In the present case, the latter possibility can be excluded with certainty.

With increase of the coverage, a second peak developed at 158–169 K; this corresponds to the formation of a multilayer of H_2O. The zero-order desorption energy of this peak (α), 43 kJ/mol, is in good agreement with the value obtained for the desorption of multilayer H_2O from other metals, e.g. on Pt(111) [8], Ni(111) [25], Pd(100) [15], Cu(110) [33], Ru(001) [19] and Ir(110)

[20] surfaces. This agreement suggests that the desorption energy is independent of the metal and is related to the sublimation energy of ice, ~ 50 kJ/mol.

We can assume that, similarly to the other metals, H_2O is bound to the Rh(111) via one of the lone pair orbitals and the second lone pair orbital is used for hydrogen bonding to adjacent H_2O [11,12,17,19,21,27]. The formation of the multilayer may occur on top of this primary layer. The surface concentration for the first layer (β state) at saturation is (within an accuracy of $\pm 50\%$) $\sim 3 \times 10^{14}$ H_2O molecules/cm^2, which corresponds to a surface coverage of $\theta = 0.19$ relative to the number of surface metal atoms, i.e. 1.59×10^{15} atoms/cm^2. This value is almost the same as that for Pd(100) [15], but considerably less than those for Pt(111) [8], Ru(001) [19] and Re surfaces [21].

The adsorption of H_2O on a Rh(111) surface at 110 K produced new losses at 8.4, 10.5 and 14–14.5 eV in the electronic range in the EEL spectrum. At low exposures, where mainly the chemisorbed phase is present, only one peak developed at 14–14.5 eV. The peaks at 8.4 and 10.5 eV appeared when the multilayer phase was formed at higher exposures.

When Rh(111) exposed to H_2O at 110 K was heated, the 8.4 and 10.5 eV losses were eliminated by 175 K, while the 14 eV loss vanished at around 201 K. These values are in accord with the thermal desorption data for the multilayer and the chemisorbed state (fig. 2), supporting our view that the 14 eV loss is caused by chemisorbed H_2O, while the three-peak structure, at 8.4, 10.5 and 14 eV, is due to formation of the multilayer. It is important to mention that no other losses developed in the EELS of Rh(111), even on high H_2O exposure (~ 100 L) and/or at the higher temperature of 300 K.

To establish the origin of the above losses, it is helpful to consider that the highest occupied orbitals in the free H_2O molecule are at 17.17 eV ($1B_2$), 13.15 eV ($3A_1$) and 11.68 eV ($1B_1$) below the vacuum level [46]. These orbitals are measured in UPS for the adsorbed H_2O molecule on clean metals at 6.5–7.4, 9.0–9.5 and 12.2–13.7 eV referenced to the Fermi level [13,26,33]. The fact that we found three losses for adsorbed H_2O in the EEL spectrum of Rh fits in well with this picture. Accordingly, we tentatively assign the 8.4, 10.5 and 14 eV losses to the intramolecular electronic excitation from $1B_1$, $3A_1$ and $1B_2$, respectively, to the unoccupied $4A_1$ orbital of H_2O, which is situated near above the Fermi level. The appearance of the loss at ~ 14 eV ($1B_2 \rightarrow 4A_1$) in the chemisorbed state also indicates that the H_2O is adsorbed as a molecule, as the $1B_2$ provides the bond between the hydrogen and oxygen holding the molecule together [13].

4.2. H_2O adsorption and desorption from clean and from boron-contaminated Rh foil

The main characteristics of H_2O adsorption and desorption for a clean polycrystalline Rh foil, as established by TDS and EELS measurements, agreed quite well with those for clean Rh(111). However, when boron was allowed to segregate onto the surface, significant differences were observed. Although the amount of H_2O adsorbed in the β state increased only slightly with increase of the boron impurity level, as indicated by the higher intensity of the 14 eV loss, less H_2O desorbed in the β state. The peak temperature, $T_p = 185$ K, however, remained unaltered. Completely new features were the formation of adsorption states with $T_p = 320$ K and 370 K, and the formation of H_2 with $T_p = 367$ K. The latter indicated that adsorbed H_2O underwent dissociation on the boron-containing Rh surface. The amount of H_2 increased with the relative intensity of the boron Auger signal, but a linear correlation was not found. At a high boron concentration, $R_B = 0.08$, almost ~ 25% of chemisorbed H_2O dissociated on the surface.

The drastic effect of boron impurity on the behaviour of H_2O on Rh exhibited in the EEL spectra. Although the same losses appeared in the EEL spectra of clean and boron-contaminated Rh foil following H_2O adsorption to 110 K, and they exhibited the same thermal behaviour as that observed for the Rh(111) surface, a new loss developed at 9.4 eV at about 270 K. This showed maximum intensity at 650 K and disappeared only above 950 K.

In order to assign this loss to a particular surface species, the interaction of O_2 was also investigated by EEL spectroscopy [47]. On clean Rh surfaces the adsorption of O_2 apparently intensified only the intrinsic loss of Rh at 5–6 eV, and produced no other detectable losses, even at higher exposure at 100 or 300 K. In the presence of boron impurity, however, an intense new loss appeared at 9.4 eV. This was detected first at 200 K; it exhibited an identical temperature-dependence to that of the 9.4 eV loss produced by H_2O adsorption on the same surface.

The 9.4 eV loss also appeared when the boron-contaminated Rh surface was exposed to CO_2 at or above 300 K [37,38]. When all these observations are taken into account, it seems plausible that the 9.4 eV loss is due to the formation of some kind of boron-oxide surface species.

The conclusion is supported by the EELS study of the interaction of polycrystalline boron with oxygen [48]. The most intense loss was found at 8.6 eV. Its intensity markedly increased with the oxygen exposure. We note here that boron was found to be resistant to oxidation by traditional UHV exposure techniques. Therefore O_2 was introduced into the system through the ionizer of a sputter ion gun [48]. The comparison of the two systems illustrates the higher reactivity of boron in the surface layer of Rh and/or the importance of the Rh matrix in the surface reaction.

The formation of the B–O species is also supported by high-resolution Auger spectroscopic measurements. After the adsorption of H_2O at above 270 K, two new Auger transitions appeared at 157 and 168–172 eV. At the same time, the intensities of the elemental boron Auger signals at 179 and 182 eV decreased. These features are very similar to those observed following the oxidation of polycrystalline boron [48] and can be attributed to the formation of B_2O_3 [49,50]. A somewhat similar change in the structure of the boron Auger signals was registered on the adsorption of O_2 on boron-contaminated Rh surface [47,51]. In the case of H_2O adsorption, the intensities of the "oxide-like" Auger transitions relative to the elemental boron feature were less than after O_2 adsorption at saturation. This indicates that only part of the boron is involved in the dissociation of H_2O.

The formation of a compound, boron oxide, is revealed by the position of the oxygen Auger signal. In the case of a clean Rh surface, the oxygen Auger feature appears at 520 eV; on the boron-contaminated Rh, however, the adsorption of H_2O and O_2 produces an Auger feature at 513.7 eV.

These results indicate that H_2O dissociates on boron-contaminated Rh surfaces, producing adsorbed H and boron-oxide species. The driving force of this surface reaction is the high stability of the B–O bond; the dissociation energy of this bond is 787 kJ/mol [52].

As regards the dissociation of chemisorbed H_2O, we propose the following reaction sequences. It is reasonable to assume that the boron interacting with adsorbed H_2O via a lone pair electron of the oxygen atom of the H_2O molecule:

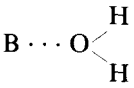

$$\mathrm{B\cdots O}\begin{matrix}\diagup \mathrm{H}\\ \diagdown \mathrm{H}\end{matrix} \tag{A}$$

exerts a stabilizing effect on it. This feature is apparently exhibited in the thermal desorption of H_2O; new adsorption states are formed with $T_p = 320$ and 370 K. The amount of H_2O desorbed in these states is very small, $\sim 1 \times 10^{13}$ H_2O molecules/cm^2; which is probably due to the fact that the H_2O molecule is bound so strongly to the boron that, instead of desorbing, it mainly dissociates. However, the existence of stabilized H_2O was not seen in the EEL spectra as the characteristic low for chemisorbed H_2O ($\sim$ 14 eV) was detected only up to 210 K. This could be due to the low concentration of species (A) on the surface. An alternative explanation is that decomposition of this surface complex occurred around 200 K:

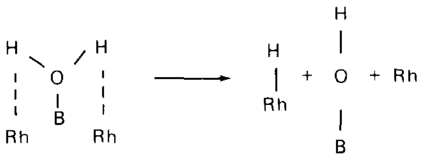

producing B–OH and Rh–H species.

As the 9.4 eV loss attributed to the B–O species was first detected at 270 K, we may conclude that the dissociation of chemisorbed H_2O, or the disproportionation of B–OH species,

$$2\ B\text{–}OH = 2\ B\text{–}O + H_2O$$

starts at around this temperature, and occurs at maximum rate above 300 K. We mention here that in the case of the Al–H_2O system the onset of this transformation of hydroxide to oxide was observed at 240 K [53]. The recombination reaction

$$B\text{–}OH + 2\ Rh\text{–}H = H_2O$$

can also occur, but this process does not lead to the formation of B–O species.

As the peak temperature for H_2 desorption from a boron-contaminated surface agreed quite well with that determined on clean Rh surfaces [42–45], we can conclude that hydrogen is bonded to the Rh, and its formation is a desorption rate limited process.

As concerns the significant changes occurring in the intensity of the 9.4 eV loss above 450 -500 K (when all the desorption processes have been completed), these have probably no connection with the surface reactions of adsorbed H_2O, as the same features were experienced following O_2 adsorption on a boron-containing Rh surface [47]. It is very likely that this behaviour is due to the transformation or polymerization of B–O into another boron-oxide species. We will deal with this process in detail elsewhere [47].

References

[1] F. Solymosi, A. Erdőhelyi and T. Tombácz, Appl. Catalysis 14 (1985) 65.
[2] J.M. Lehn, J.P. Sauvage and R. Ziessel, Nouv. J. Chim. 4 (1980) 623.
[3] J.M. Lehn, J.P. Sauvage, R. Ziessel and L. Hilaire, Israel J. Chem. 22 (1982) 168.
[4] J.M. Lehn, in: Proc. 8th Intern. Congr. on Catalysis, Vol. 1 (1984) p. 63.
[5] F. Solymosi and I. Tombácz, to be published.
[6] J.J. Zinck and W.H. Weinberg, J. Vacuum Sci. Technol. 17 (1980) 188.
[7] P.R. Norton, J. Catalysis 36 (1975) 211.
[8] G.B. Fisher and J.L. Gland, Surface Sci. 94 (1980) 446.
[9] G.B. Fisher and B.A. Sexton, Phys. Rev. Letters 44 (1980) 683.
[10] L.E. Firment and G.A. Somorjai, Surface Sci. 55 (1976) 413.
[11] H. Ibach and S. Lehwald, Surface Sci. 91 (1980) 187.
[12] B.A. Sexton, Surface Sci. 94 (1980) 435.
[13] J.N. Miller, L. Lindau and W.E. Spicer, Surface Sci. 111 (1981) 595.
[14] J.R. Creighton and J.M. White, Surface Sci. 122 (1982) L648.
[15] E.M. Stuve, S.W. Jorgensen and R.J. Madix, Surface Sci. 146 (1984) 179.
[16] T.E. Madey and J.T. Yates, Jr., Chem. Phys. Letters 51 (1977) 77.
[17] P.A. Thiel, F.M. Hoffman and W.H. Weinberg, J. Chem. Phys. 75 (1981) 5556.
[18] K. Kretzschmark, J.K. Sass and A.M. Bradshaw, Surface Sci. 115 (1982) 183.
[19] D.L. Doering and T.E. Madey, Surface Sci. 123 (1982) 305.
[20] T.S. Wittrig, D.E. Ibbotson and W.H. Weinberg, Surface Sci. 102 (1981) 506.

[21] J. Jupille, P. Pareja and J. Fusy, Surface Sci. 139 (1984) 505;
J. Jupille, J. Fusy and P. Pareja, Surface Sci. 143 (1984) L433.
[22] F.P. Netzer and T.E. Madey, Surface Sci. 127 (1983) L102;
M.Q. Ding and E.M. Williams, Surface Sci. 160 (1985) 189.
[23] R.L. Stockbauer, D.M. Hanson, S.A. Flodström and T.E. Madey, J. Vacuum Sci. Technol. 20 (1982) 562.
[24] D.J. Dwyer, G.W. Simmons and R.P. Wei, Surface Sci. 64 (1977) 617.
[25] T.E. Madey and F.P. Netzer, Surface Sci. 117 (1982) 549.
[26] C. Benndorf, C. Nöbl, M. Rüsenberg and F. Thieme, Surface Sci. 111 (1981) 87.
[27] C. Benndorf, C. Nöbl and F. Thieme, Surface Sci. 121 (1982) 249;
C. Benndorf and T.E. Madey, in: Proc. ICSS-5, Madrid, 1983;
C. Nöbl, C. Benndorf and T.E. Madey, Surface Sci. 157 (1985) 29.
[28] J.L. Falconer and R.J. Madix, J. Catalysis 51 (1978) 47.
[29] J.M. Heras, H. Papp and W. Spiess, Surface Sci. 117 (1982) 590.
[30] E.M. Stuve, R.J. Madix and B.A. Sexton, Surface Sci. 111 (1981) 11.
[31] C.T. Au, J. Breza and M.W. Roberts, Chem. Phys. Letters 66 (1979) 340.
[32] C. Mariani and K. Horn, Surface Sci. 126 (1983) 279.
[33] K. Bange, D.E. Grider, T.E. Madey and J.K. Sass, Surface Sci. 137 (1984) 39.
[34] A. Berkó, Thesis, University of Szeged (1983).
[35] F. Solymosi and L. Bugyi, Appl. Surface Sci. 21 (1985) 125.
[36] J. Kiss and F. Solymosi, Surface Sci. 135 (1983) 243.
[37] F. Solymosi and J. Kiss, Chem. Phys. Letters 110 (1984) 639.
[38] F. Solymosi and J. Kiss, Surface Sci. 149 (1985) 17.
[39] C.M. Chan, R. Aris and W.M. Weinberg, Appl. Surface Sci. 1 (1978) 360.
[40] F. Solymosi and L. Bugyi, Surface Sci. 147 (1984) 685.
[41] F. Solymosi and A. Berkó, Surface Sci. 141 (1984) 533.
[42] J.T. Yates, Jr., P.A. Thiel and W.H. Weinberg, Surface Sci. 84 (1979) 427.
[43] V.J. Mimeault and R.S. Hansen, J. Chem. Phys. 45 (1966) 2240.
[44] D.G. Gastner, B.A. Sexton and G.A. Somorjai, Surface Sci. 71 (1978) 519.
[45] F. Solymosi and J. Kiss, J. Catalysis 81 (1983) 95.
[46] W.L. Jorgensen and L. Salem, The Organic Chemist's Book of Orbitals (Academic Press, New York, 1973).
[47] J. Kiss and F. Solymosi, to be published.
[48] J.W. Rogers, Jr. and M.L. Knotek, Appl. Surface Sci. 13 (1982) 352.
[49] D.J. Joyner and D.M. Hercules, J. Chem. Phys. 72 (1980) 1095.
[50] G. Hanke and K. Müller, Surface Sci. 152/153 (1985) 902.
[51] S. Semancik, G.L. Haller and J.T. Yates, Jr., Appl. Surface Sci. 10 (1982) 546.
[52] B. deB. Darwent, Natl. Stand. Ref. Data Ser., Natl. Bur. Stand. (US) 31 (1970).
[53] J.C. Fuggle, L.M. Watson, D.J. Fabian and S. Affrossman, Surface Sci. 49 (1975) 61.